Japanese Journal of Ophthalmology (2019) 63:457–466
https://doi.org/10.1007/s10384-019-00691-6

THE OFFICIAL INTERNATIONAL JOURNAL OF THE JAPANESE OPHTHALMOLOGICAL SOCIETY

CLINICAL INVESTIGATION

Macular vessel density in untreated normal tension glaucoma with a hemifield defect

Nozomu Uchida[1,2] · Kyoko Ishida[2] · Ayako Anraku[2] · Asuka Takeyama[2,3] · Goji Tomita[2]

Received: 16 January 2019 / Accepted: 30 August 2019 / Published online: 17 October 2019
© Japanese Ophthalmological Society 2019

Abstract

Purpose To investigate macular vessel density (MVD) and structural alterations in untreated normal tension glaucoma (NTG) with a hemifield defect (HFD) and to compare these with the findings in healthy eyes.

Study design Case series with a healthy group for comparison.

Methods Thirty-four eyes of 34 untreated NTG patients with HFD and 28 eyes of 28 healthy subjects were enrolled. RTVue-XR Avanti^{TM} (Optovue, Inc.), a combined OCT-A and SD-OCT system, was used to determine MVD and inner macular thickness (IMT) measurements. Mean circumpapillary retinal nerve fiber (cpRNFL) and macular ganglion cell complex (mGCC) thicknesses were measured with the RTVue-100^{TM} (Optovue, Inc.). Wilcoxon signed-rank test was used to evaluate differences between defective and normal hemifields in NTG eyes and Mann–Whitney U test to evaluate differences between normal hemifields in NTG eyes and healthy eyes.

Results In comparison with healthy eyes, the normal hemifields of NTG eyes showed significantly reduced MVD, as well as cpRNFL and mGCC thicknesses, although IMT did not differ between the two groups. The defective hemifield in NTG eyes showed significantly reduced IMT, as well as cpRNFL and mGCC thicknesses, compared with the normal hemifield, although MVD did not differ between the two hemifields.

Conclusion Hemodynamic deficiencies and structural damage might have already begun in the perimetrically normal hemifields of NTG eyes. Further studies are needed to elucidate whether the reduction in MVD may precede structural changes or the reduction in vasculature and structural loss may vary with disease severity in at least in some cases.

Keywords Optical coherence tomography angiography · Normal tension glaucoma · Macular vessel density · Hemifield defect

Introduction

Normal tension glaucoma (NTG) is a chronic optic neuropathy characterized by progressive loss of retinal ganglion cells (RGCs) and their axons, resulting in structural damage to the inner retina and optic nerve head (ONH) along with irreversible visual field (VF) damage [1–3]. Although the pathogenesis of NTG remains unclear, intraocular pressure (IOP) and vascular factors may contribute to NTG [2–6].

Spectral-domain optical coherence tomography (SD-OCT), which can measure retinal thickness, is frequently used in the diagnosis and management of glaucoma. OCT angiography (OCT-A) has been recently developed to detect the changes in OCT signals caused by flowing red blood cells in blood vessels. The OCT-A technique can provide reproducible quantitative assessment of the retinal and optic disc blood flow [7]. Recent studies using OCT-A document

Corresponding Author: Kyoko Ishida

✉ Kyoko Ishida
kyoko.ish@gmail.com

[1] Department of Ophthalmology, Toho University Graduate School of Medicine, Tokyo, Japan

[2] Department of Ophthalmology, Toho University Ohashi Medical Center, 2-22-36 Ohashi, Meguro-ku, Tokyo 153-8515, Japan

[3] Department of Ophthalmology, Teikyo University School of Medicine, University Hospital Mizonokuchi, Kawasaki, Japan

microvascular dropout in the optic nerve, peripapillary retina, and macula in glaucomatous eyes [7–10]. Nevertheless, it is unknown whether the microvascular changes in glaucoma are a primary event or the result of RGC degeneration. Although longitudinal OCT-A studies are needed to elucidate the pathology of NTG, such studies provide limited information because OCT-A is a relatively new technique [11–13]. Alternative approaches include cross-sectional studies, which have assessed preperimetric glaucoma (PPG) or glaucoma with hemi field defects (HFD) [9–12, 14–19].

In glaucomatous eyes with a single HFD, reduced thicknesses of both the retinal nerve fiber layer (RNFL) and macular ganglion cell complex (mGCC) have been detected, even in perimetrically intact hemifields [11, 16–18, 20, 21]. The macula has the greatest density of RGCs; thus, it is important for detection of early structural changes in glaucoma [22, 23]. Because retinal capillary plexuses support the high metabolic needs of RGCs in the macular region, macular vessel density (MVD) may be an essential indicator [23]. However, to our knowledge, few studies have used OCT-A to evaluate MVD in glaucomatous eyes with HFD [11, 18], while none have assessed patients with NTG.

Here, in order to investigate the relationships between vessel density and other parameters, we measured the MVD by using OCT-A, and we also assessed the RNFL, mGCC, and inner macular thickness (IMT) by SD-OCT in the eyes of healthy patients and in NTG patients with HFD.

Materials and methods

Study subjects

Data for the eyes of 36 Japanese subjects with untreated NTG with an HFD and 30 healthy control subjects who visited the eye clinic of Toho University Ohashi Medical Center from November 2015 to February 2018 were collected. The study was approved by the Ethics Committee of Toho University Ohashi Medical Center (No. H16055 and No.15-86); the opportunity of rejection was ensureded for subjects with NTG by the opt-out method on our website. Written informed consent was obtained from healthy controls; and the study was conducted according to the tenets of the Declaration of Helsinki.

NTG was defined by the presence of normal and open anterior chamber angles; glaucomatous ONH appearance with a corresponding VF defect assessed via the standard program of the Humphrey Field Analyzer (HFA, Carl Zeiss Meditec); IOP ≤ 21 mmHg on at least three different days; best-corrected visual acuity (BCVA) of at least 20/25; spherical equivalent refractive errors between -6.00 and +6.00 diopters (D); and refractive cylindrical error within 2.50 D.

Healthy participants were included if they had no family history of glaucoma, a normal-appearing ONH with an intact neuroretinal rim and RNFL, normal standard automated perimetry findings, and IOP ≤ 21 mmHg without a history of elevated IOP. We excluded subjects who had any of the following conditions: history of intraocular surgery, intraocular eye disease (other than NTG in glaucoma patients), diabetes mellitus (DM), systemic hypertension (HT), other systemic or ocular diseases known to affect refractive errors and VF, unreliable VF test results, or an inability to clinically view or photograph the optic discs due to media opacity or poorly dilating pupils.

If both eyes met all eligibility criteria, the eye with the lower mean deviation (MD) in the HFA test was selected in NTG patients. Both healthy participants and NTG patients were matched for age, gender, and spherical equivalent refractive errors.

Clinical examinations

All participants were interviewed to obtain their medical history and information regarding age and gender. Comprehensive ophthalmic examinations included assessments of refraction and BCVA, slit-lamp biomicroscopy, IOP measurements, and stereoscopic fundus examination. IOP was measured using a Goldmann applanation tonometer on the same day OCT-A measurements were obtained. Systolic blood pressure (SBP) and diastolic blood pressure (DBP) were measured before performing OCT-A measurements. Mean blood pressure (MBP) and mean ocular perfusion pressure (MOPP) were calculated. In all subjects, OCT-A and SD-OCT measurements were obtained on the same day, and VF was tested within 6 months.

Visual field analyses

Standard automated perimetry was performed with an HFA by using the 30-2 Swedish Interactive Threshold Algorithm. VF tests were considered reliable when fixation losses were <20%, false-positives were <15%, and false-negatives were <33%.

HFD in glaucomatous eyes was defined as a cluster of three or more, non-edge, contiguous points in the pattern deviation (PD) plot of an HFA with probability level <5% in either the superior or inferior hemifield (at least one of the points had a probability level <1%, and the opposite hemifield did not have a point with probability level <2%); HFD was alternatively defined as a cluster of three or more contiguous points with probability level <5%. In addition, glaucoma hemifield test results were required to be outside normal limits [20].

A normal standard automated perimetry result was defined as a glaucoma hemifield test result within normal

limits, a pattern standard deviation (PSD) within 95% confidence interval limits, and not having one point at the $P < 0.01$ level and two significant ($P < 0.05$) non-edge-contiguous points in the PD plot [20].

The total deviation (TD) plot maps of the HFA were divided into superior and inferior hemifields. To avoid rim artifacts, the 16 edge points (boxed points) were excluded from analyses (Fig. 1). Excluding the Mariotte blind spot, we calculated the average TD values of 29 stimuli, some in the superior and some in the inferior hemifield. In four central stimuli surrounded by the blue dotted line, the average central TD values of two stimuli were calculated in either the superior or inferior hemifields. In healthy control subjects, the average TD values of 58 stimuli and the average central TD values of four stimuli in both the superior and inferior hemifields were used for statistical analysis.

RNFL and GCC thickness measurements

After pupil dilation via administration of 0.4% tropicamide, a well-trained operator obtained good-quality OCT images. SD-OCT and OCT-A images were acquired by the same operator during the same visit. Figure 2 shows a representative NTG eye with inferior HFD.

Mean circumpapillary RNFL (cpRNFL) and mGCC thickness measurements were obtained with the RTVue-100 spectral-domain OCT (software version 4.0, Optovue, Inc.).

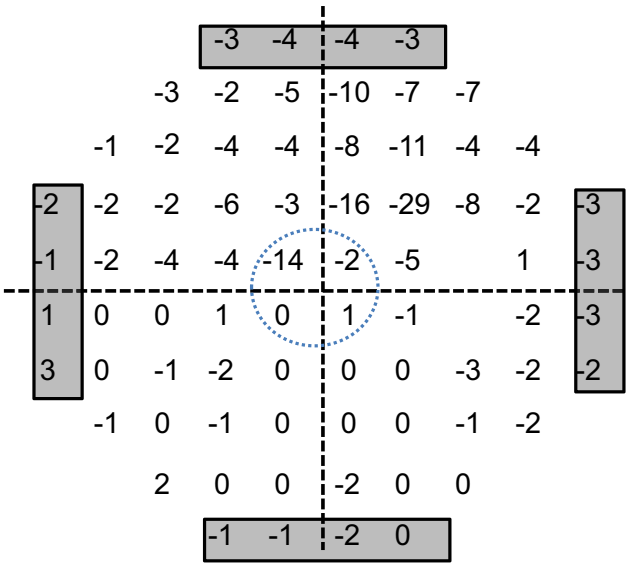

Fig. 1 The total deviation (TD) plot maps of a Humphrey Field Analyzer 30-2 Swedish interactive threshold algorithm standard. To avoid rim artifacts, the 16 edge points (boxed points) were excluded from analyses. In NTG eyes, the average TD values of 29 stimuli were calculated in either the superior or inferior hemifields. In four central stimuli surrounded by the blue dotted line, the average central TD values of two stimuli were calculated in either the superior or inferior hemifields

Using dedicated software, RNFL thickness was measured at a diameter of 3.45 mm around the center of the optic disc. Average cpRNFL thickness of the superior and inferior hemifields was automatically measured (Fig. 2c).

A GCC scanning protocol was used to determine mGCC thickness (Fig. 2d). To achieve optimal coverage within the temporal region, the GCC protocol scan was centered 1 mm temporal to the fovea and a 6 × 6 mm map was created. The mGCC thickness was measured from the internal limiting membrane (ILM) to the outer inner plexiform layer (IPL) boundary; the OCT system provided overall superior and inferior hemifield averages. Images were excluded from analyses when the signal strength index was low (<40), segmentation errors occurred, or when the scan circle was not centered at the optic disc.

Vessel density measurements

The RTVue-XR Avanti with AngioVue software (Optovue, Inc., version 2015.100.0.35) consists of a combined OCT-A and SD-OCT system. The instrument used for OCT-A imaging was based on the AngioVue Imaging System for obtaining amplitude-decorrelation angiography images. The Angio macular protocol dedicated software, provided by Optovue (AngioAnalytics^{TM}), was used for flow density analysis. Vessel density was defined as the percentage area occupied by the vessel, measured using the intensity-based thresholding feature of the software, through a previously reported calculation method [8].

The parafoveal vessel density from the macula scan yielded measurements in an annular region with an inner diameter of 1 mm and an outer diameter of 3 mm centered on the fovea. Each scan was automatically segmented to visualize superficial retinal capillary plexuses and deep retinal capillary plexuses of the retina. For this analysis, the MVD of superficial retinal capillary plexuses, measured from 3 μm below the ILM to 15 μm below the IPL, was used. Parafoveal vessel density was originally divided into four sectors of 90 degrees each (superior, temporal, inferior, and nasal); the upper and lower sectors were used for the analysis (Fig. 2e).

Images with poor quality, defined by the following criteria, were excluded from analysis: signal strength indicator < 45 due to media opacity, poor clarity, motion artifacts that were visible as an irregular vessel pattern on the en-face angiogram, or off-centered fovea.

Inner macular thickness measurements

All subjects underwent macular cube imaging with a commercially available SD-OCT system provided by RTVue-XR Avanti with AngioVue. The inherent GCC scanning protocol was used to measure "central" macular GCC thickness, consisting of the RNFL, ganglion cell layer, and IPL, for

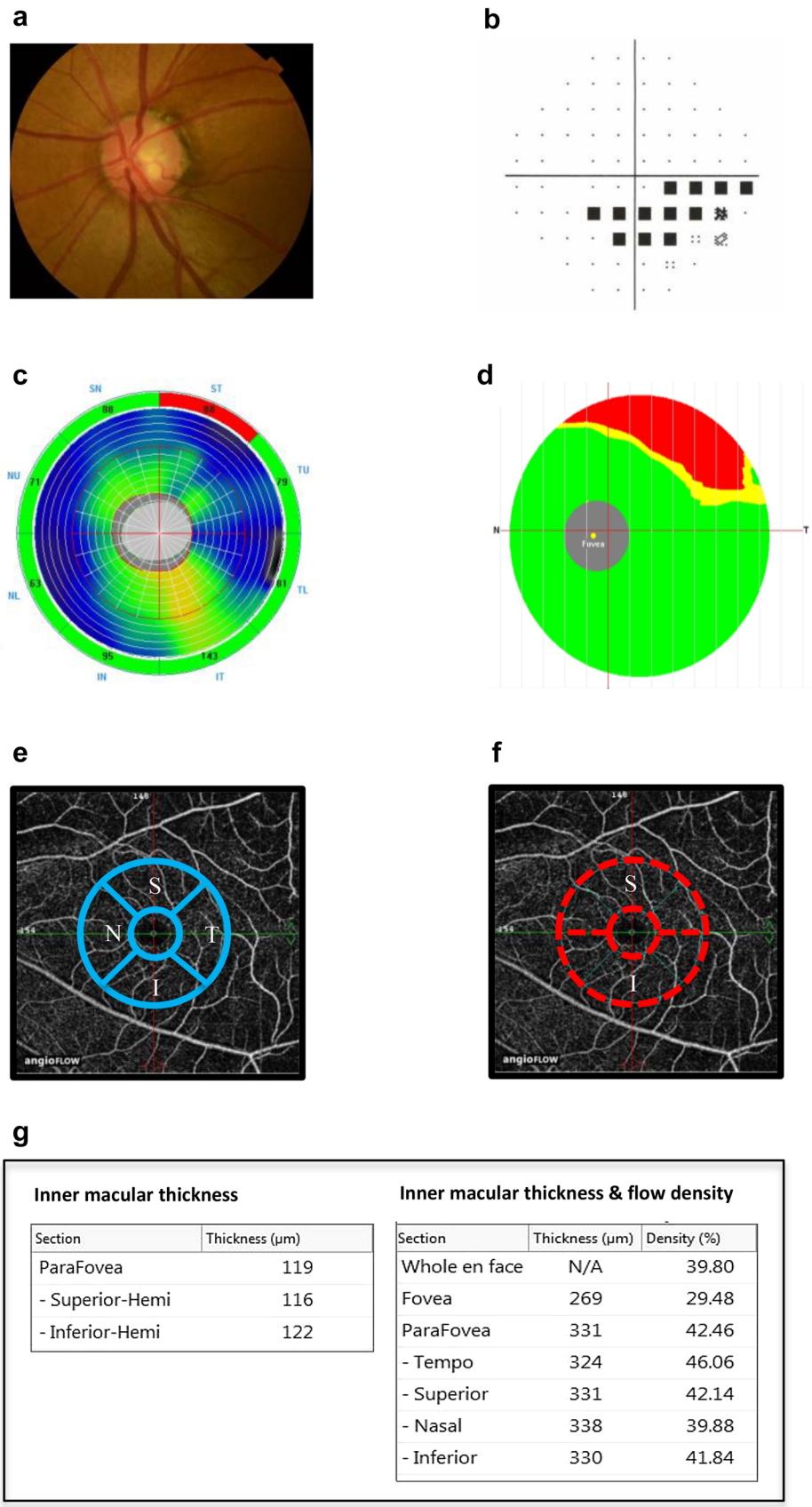

Fig. 2 A representative glaucomatous eye with inferior visual field defect. a, Optic nerve head photograph shows rim thinning and retinal nerve fiber layer (RNFL) defects at the superior-temporal region. b, Total deviation map of the Humphrey Field Analyzer 30-2 SITA standard shows inferior visual field defects. c, RNFL thickness was measured with RTVue-100 spectral-domain OCT at a diameter of 3.45 mm around the center of the optic disc. Circumpapillary RNFL thickness map shows thinning at the superior-temporal region. d, Macular ganglion cell complex (GCC) thickness was measured with the RTVue-100 spectral-domain OCT. The GCC protocol scan was centered 1 mm temporal to the fovea and a 6 × 6 mm map was created. The GCC map shows thinning at the superior region. e, Vessel density map of the superficial retinal layer obtained using RTVue-XR Avanti with AngioVue shows capillary dropout at the superior region. The macula scan yields measurements in an annular region with an inner diameter of 1 mm and an outer diameter of 3 mm centered on the fovea (Blue line). Each scan was automatically segmented to visualize superficial retinal capillary plexuses. Parafoveal vessel density was originally divided into four sectors of 90 degrees each (S; superior, T; temporal, I; inferior, and N; nasal); superior and inferior sectors were used for the analysis. f, The macula scan yields measurements in an annular region with an inner diameter of 1 mm and an outer diameter of 3 mm centered on the fovea. The inner macular thickness (IMT) was originally divided into two sectors (red dotted line), and the superior (S) and inferior (I) sectors were used for the analysis. g, Summary of the measurements obtained with the RTVue-XR Avanti with AngioVue. In this case, superior IMT and superior parafoveal macular vessel density were 116 μm and 42.14%, respectively

which the measurement depth was identical to that for MVD (Fig. 2f).

To differentiate this measurement from the mGCC thickness measurement with the RTVue-100 SD-OCT, which uses a 6 × 6 mm map centered 1 mm temporal to the fovea, we designated the "central" GCC thickness measured via the RTVue-XR Avanti as IMT in this study. The IMT was measured in an annular region with an inner diameter of 1 mm and an outer diameter of 3 mm centered on the fovea. The IMT was originally divided into two sectors, and the superior and inferior sectors were used for the analysis (Fig. 2f). Only good-quality images were included (i.e., those with signal strength index > 45 and without segmentation errors or artifacts).

Statistical analysis

The normality of the data was examined using the Shapiro-Wilk test, and non-parametric tests were performed for non-normally distributed data. Comparisons between healthy and glaucomatous eyes were performed using the Mann–Whitney *U* test for continuous data and the chi-squared test for categorical data. Comparisons between normal and defective hemifields of glaucomatous eyes were performed using Wilcoxon signed-rank test. Multiple regression analyses were used to determine factors related to the vessel density. Statistical significance was accepted at $P < 0.05$. All analyses were performed using statistical software (SPSS version 19.0 for Windows; SPSS Inc.).

Results

The demographic and clinical characteristics of the 28 healthy participants and 34 NTG patients are presented in Table 1. There were no significant differences between the healthy participants and glaucoma patients in age, gender, spherical equivalent refraction, MOPP, or systemic variables (SBP, DBP, and MBP) (all *P* values > 0.05). As expected, NTG eyes showed worse VF on average, with lower MD and higher PSD values, thinner cpRNFL and mGCC, reduced IMT, and smaller MVD in comparison with healthy eyes (*P* values < 0.05). Although NTG subjects were untreated, their IOP was higher than in normal participants ($p = 0.045$). The average temporal quadrant vessel density in healthy participants was 50.46% and in glaucoma patients 48.52%; the nasal quadrant vessel density in healthy patients was 47.78% and in glaucoma patients, 46.00%. There was a statistically significant difference in temporal vessel density ($p = 0.019$) between healthy participants and glaucoma patients, but not in nasal vessel density ($p = 0.053$). Twenty-one patients had superior HFD and 13 had inferior HFD in the NTG eyes.

A summary of the TD and OCT measurements corresponding to the normal and defective hemifields of the NTG patients and those in healthy eyes is shown in Table 2.

Table 1 Demographic and ocular characteristics of the study subjects

	Healthy eyes N=28	Glaucomatous eyes N=34	*P*
Age (years)	48.0 ± 10.6	51.8 ± 12.5	0.205*
Gender (male/female)	14/14	14/20	0.487†
Spherical equivalent (D)	-1.7 ± 2.0	-2.5 ± 2.3	0.172*
Mean deviation (dB)	-0.3 ± 1.4	-3.7 ± 3.2	**< 0.001***
Pattern standard deviation (dB)	1.6 ± 0.5	6.7 ± 5.1	**< 0.001***
IOP (mmHg)	14.4 ± 2.0	16.0 ± 3.3	**0.045***
MOPP (mmHg)	45.8 ± 5.9	46.7 ± 9.7	0.888*
SBP (mmHg)	118.0 ± 11.8	126.0 ± 16.7	0.065*
DBP (mmHg)	76.5 ± 8.9	78.1 ± 15.9	0.713*
MBP (mmHg)	90.4 ± 9.2	94.0 ± 15.2	0.384*
cpRNFL (μm)	94.9 ± 8.1	81.2 ± 9.1	**< 0.001***
mGCC (μm)	96.5 ± 5.3	83.4 ± 7.9	**< 0.001***
Inner macular thickness (μm)	120.4 ± 8.0	114.0 ± 9.9	**0.007***
Macular vessel density (%)	49.5 ± 4.8	45.4 ± 4.6	**0.002***

The data are presented as means ± standard deviations

*Differences between groups were assessed using analysis of variance with the Mann–Whitney U test

†Differences between groups were analyzed using $\chi 2$ tests

IOP, intraocular pressure; MOPP, mean ocular perfusion pressure; SBP, systolic blood pressure; DBP, diastolic blood pressure; MBP, mean blood pressure; cpRNFL, circumpapillary retinal nerve fiber layer; mGCC, macular ganglion cell complex

Numbers written in boldface are statistically significant ($P < 0.05$)

Table 2 Total deviations and optical coherence tomography measurements corresponding to the normal and defective hemifields and those in healthy eyes

	Healthy eyes (N=28)	Glaucomatous eyes (N=34)		*P	†P	‡P
		Normal hemifield	Defective hemifield			
Average TD (dB)	-0.3± 1.4	-0.7 ± 1.2	-6.2 ± 5.8	0.151	**< 0.001**	**< 0.001**
Central average TD (dB)	0.6 ± 1.3	-0.2 ± 1.1	-5.0 ± 8.4	**0.010**	**< 0.001**	**< 0.001**
cpRNFL (μm)	94.7 ± 8.1	88.9 ± 10.4	73.7 ± 10.5	**0.008**	**< 0.001**	**< 0.001**
mGCC (μm)	96.5 ± 5.3	91.6 ± 7.7	75.0 ± 9.9	**0.005**	**< 0.001**	**< 0.001**
Macular vessel density (%)	49.5 ± 4.8	46.0 ± 5.1	44.8 ± 4.9	**0.011**	0.110	**0.001**
Inner macular thickness (μm)	120.4 ± 8.0	117.0 ± 8.7	111.0 ± 12.9	0.085	**< 0.001**	**0.001**

The data are presented as means ± standard deviations

*Comparisons between healthy eyes (N=28) and the normal hemifields of glaucomatous eyes (N=34)

†Comparisons between the normal and the defective hemifields of glaucomatous eyes (N=34)

‡Comparisons between healthy eye (N=28) and the defective hemifields of glaucomatous eyes (N=34)

Statistical significance determined with Wilcoxon signed-rank test

TD, total deviation; cpRNFL, circumpapillary retinal nerve fiber layer; mGCC, macular ganglion cell complex

Numbers written in boldface are statistically significant ($P < 0.05$)

The cpRNFL ($P = 0.008$) and mGCC ($P = 0.005$) thicknesses and MVD ($P = 0.011$) were significantly smaller in the normal hemifields of NTG eyes than in healthy eyes, although average TD ($P = 0.151$) and IMT ($P = 0.085$) did not significantly differ between the two groups. According to Anderson-Patela's criteria, hemifields opposite the defective areas in NTG eyes are considered to be perimetrically normal; however, central average TD was significantly lower in these hemifields than in those of healthy subjects.

In comparisons of the two hemifields in NTG eyes (N = 34), the defective hemifields demonstrated VF loss with lower average TD and central average TD values (both P values < 0.001), in comparison with the perimetrically normal hemifields. Although MVD did not differ between the two hemifields in glaucomatous eyes ($P = 0.110$), mGCC and cpRNFL thicknesses and IMT were significantly lower in the defective hemifields than in the normal hemifields (all P values < 0.001). As expected, all parameters showed smaller values in the defective hemifields of glaucomatous eyes than in the normal hemifields of healthy eyes (all P values < 0.001).

Table 3 shows the correlations between OCT measurements and TDs in the perimetrically normal hemifields of 34 NTG eyes. Average TD, central average TD, and MVD were not significantly correlated with any of the parameters. IMT was significantly correlated with mGCC ($r = 0.727$, $P < 0.001$) and cpRNFL ($r = 0.450$, $P = 0.008$) thicknesses.

Correlations between OCT measurements and TDs in the defective hemifields of 34 glaucomatous eyes are demonstrated in Table 4. Central average TD was significantly correlated with mGCC thickness ($r = 0.487$, $P = 0.004$) and IMT ($r = 0.355$, $P = 0.039$). MVD was not significantly correlated with any of the parameters. IMT was significantly correlated with mGCC ($r = 0.738$, $P < 0.001$) and cpRNFL ($r = 0.426$, $P = 0.012$) thicknesses.

Table 5 shows correlations between OCT measurements and TDs in all subjects (n=62). Average TD was significantly correlated with mGCC ($r = 0.515$, $P < 0.001$)

Table 3 Correlations between optical coherence tomography measurements and total deviations in the normal hemifields of glaucomatous eyes (N=34)

	mGCC		cpRNFL		Macular vessel density		Inner macular thickness	
	r	P	r	P	r	P	r	P
Average TD	-0.015	0.933	0.015	0.931	0.080	0.654	0.056	0.752
Central average TD	0.005	0.977	-0.114	0.522	0.257	0.142	-0.102	0.564
Macula vessel density	0.067	0.708	0.336	0.052	N/A	N/A	-0.290	0.096
Inner macular Thickness	0.727	**< 0.001**	0.450	**0.008**	-0.290	0.096	N/A	N/A

TD, total deviation; mGCC, macular ganglion cell complex; cpRNFL, circumpapillary retinal nerve fiber layer; r, Spearman rank correlation coefficient

Numbers written in boldface are statistically significant ($P < 0.05$)

and cpRNFL ($r = 0.567$, $P < 0.001$) thicknesses. Central average TD was significantly correlated with mGCC ($r = 0.616$, $P < 0.001$) and cpRNFL ($r = 0.557$, $P < 0.001$) thicknesses, and IMT ($r = 0.410$, $P = 0.001$). MVD was significantly correlated with mGCC ($r = 0.364$, $P = 0.004$) and cpRNFL ($r = 0.473$, $P < 0.001$) thicknesses. IMT was significantly correlated with mGCC ($r = 0.730$, $P < 0.001$) and cpRNFL ($r = 0.510$, $P < 0.001$) thicknesses.

Among explanatory variables, including IOP, average TD, central average TD, mGCC and cpRNFL thicknesses, and IMT, cpRNFL thickness was a significant contributing factor for MVD (slope, 0.225; β = 0.484, 95% confidence interval [CI], 0.120–0.330; p < 0.001) in all subjects (Table 6).

Discussion

In the current study, the MVD obtained by OCT-A as well as SD-OCT parameters and TDs of VF were analyzed in both healthy and NTG eyes with HFD. To our knowledge, there are no reports discussing the assessment of MVD by using OCT-A in NTG eyes with a single HFD.

In comparison with healthy eyes, perimetrically normal hemifields of NTG eyes showed reduced mGCC and cpRNFL thicknesses. Our results agree with those of previous studies [11, 16–21]. Similarly, MVD in our study was significantly reduced in the perimetrically intact hemifields of NTG eyes, in comparison with the normal VFs of healthy subjects. Similar results are reported with Doppler OCT

Table 4 Correlations between optical coherence tomography measurements and total deviation in defective hemifields of glaucomatous eyes (N=34)

	mGCC		cpRNFL		Macular vessel density		Inner macular thickness	
	r	*P*	r	*P*	r	*P*	r	*P*
Average TD	0.221	0.210	0.291	0.095	-0.197	0.265	-0.031	0.862
Central average TD	0.487	**0.004**	0.330	0.057	0.114	0.521	0.355	**0.039**
Macular vessel density	0.119	0.504	0.321	0.064	N/A	N/A	0.144	0.416
Inner macular Thickness	0.738	**<0.001**	0.426	**0.012**	0.144	0.416	N/A	N/A

TD, total deviation; mGCC, macular ganglion cell complex; cpRNFL, circumpapillary retinal nerve fiber layer; r, Spearman rank correlation coefficient

Numbers written in boldface are statistically significant ($P < 0.05$)

Table 5 Correlations between optical coherence tomography measurements and total deviation in all subjects (N=62)

	mGCC		cpRNFL		Macular vessel density		Inner macular thickness	
	r	*P*	r	*P*	r	*P*	r	*P*
Average TD	0.515	**<0.001**	0.567	**<0.001**	0.195	0.129	0.233	0.082
Central average TD	0.616	**<0.001**	0.557	**<0.001**	0.211	0.100	0.410	**0.001**
Macula vessel density	0.364	**0.004**	0.473	**<0.001**	N/A	N/A	0.115	0.373
Inner macular thickness	0.730	**<0.001**	0.510	**<0.001**	0.115	0.373	N/A	N/A

TD, total deviation; mGCC, macular ganglion cell complex; cpRNFL, circumpapillary retinal nerve fiber layer; r, Spearman rank correlation coefficient

Numbers written in boldface are statistically significant ($P < 0.05$)

Table 6 Multiple regression analysis to determine factors contributing to macular vessel density

Analysis group	Dependent variable	Contributing variables	β	Slope	Confidence interval	*P*
Normal hemifields of NTG eyes (N=34)	Macular vessel density	none				
Defective hemifields of NTG eyes (N=34)	Macular vessel density	none				
All subjects (N=62)	Macular vessel density	cpRNFL	0.484	0.225	0.120-0.330	**<0.001**

NTG, normal tension glaucoma; cpRNFL, circumpapillary retinal nerve fiber layer; TD, total deviation; mGCC, macular ganglion cell complex; IOP, intraocular pressure

Explanatory variables: IOP. average TD, central average TD, mGCC, cpRNFL, macular inner thickness

Numbers written in boldface are statistically significant ($P < 0.05$)

[21]. Yarmohammadi et al. [18] found reduced MVD with OCT-A and reduced RNFL and mGCC thickness in the perimetrically intact hemiretinas of open angle glaucomatous eyes with a single-hemifield defect. These findings suggest that the hemodynamic deficiencies in the macular region and structural damage might have already begun in the perimetrically normal hemifields of glaucomatous eyes, including eyes with NTG. However, it remains unclear whether microvascular changes are a primary event or the result of RGC degeneration.

In comparison with the measurements in healthy eyes, the MVD measured by the RTVue-XR Avanti (a combined OCT-A and SD-OCT system) was significantly lower in the normal hemifields of the glaucomatous eye, although IMT measured by the same instrument did not significantly differ between the two groups. One possible assumption from our findings is that in the very early stages of the disease the reduction in vessel density precedes structural changes in the macular region, at least in some cases. This assumption might agree with the findings of a previous study using the same Avanti AngioVue system, in which MVD is reported to show better diagnostic accuracy than IMT in differentiating suspected glaucoma and healthy eyes [14]. Moreover, in comparison with normal eyes, Chen et al. [16] found a lower blood flux index and vessel area density in the normal hemisphere of glaucomatous eyes, whereas there was no difference in RNFL thickness between the normal VF in healthy subjects and the normal hemisphere of glaucomatous eyes. A recent longitudinal study observed a reduction in the MVD in eyes without detectable mGCC changes [12]. Hou et al. [19] report that patients with suspected bilateral glaucoma showed significantly greater inter-eye asymmetry in vessel density than bilaterally healthy eyes, but there were no significant differences in the inter-eye asymmetry for thickness parameters between the two groups. Eyes with bilateral glaucoma showed significantly greater inter-eye asymmetry both in vessel density and thickness parameters than bilateral healthy eyes. If the decrease in vessel density happens in the early stage of glaucoma, then asymmetry develops earlier [19]. These findings may support the notion that microvascular change may be a primary event at least in some cases.

Another possibility based on our findings is that the sensitivity of IMT for detection of changes applied in the current study may be inferior to other parameters such as mGCC and cpRNFL thicknesses. The measurement depths for the IMT and MVD were identical, but the measurement widths were not. That was because IMT is significantly correlated with mGCC and cpRNFL thicknesses in both the normal and the abnormal hemifields of glaucomatous eyes and in the total subject population. However, only the cpRNFL, mGCC thicknesses and MVD were significantly smaller in the normal hemifields of NTG eyes than in healthy eyes, with no differences in IMT.

To clarify whether microvascular changes may be a primary event at least in some cases or are caused by RGC death, further longitudinal studies that adapt identical measurement areas would be needed for OCT-A, mGCC, and IMT assessments.

In the current study, MVD in glaucomatous eyes differences' between normal and defective hemifields were not significant, despite the differences in IMT, mGCC and cpRNLF thicknesses between the two hemifields. Pentendo et al. [14] compared MVD and mGCC thickness in healthy individuals (MD = 0.02 dB) and patients with suspected glaucoma (MD = -0.35 dB), mild glaucoma (MD = -2.39 dB), and moderate/severe glaucoma (MD = -13.10 dB); they report that MVD was 54.9%, 52.1%, 51.8%, and 47.7%, respectively. The MVD was significantly different between groups, except between patients with suspected glaucoma and those with mild glaucoma. On the other hand, mGCC thicknesses were significantly different between groups, except between normal participants and patients with suspected glaucoma. That study further mentions that the AUROC for differentiating suspected glaucoma and healthy eyes is greater for MVD when compared with GCC thickness [14]. Hou et al. [15] compared MVD and GCC thickness in healthy individuals (MD = 0.05 dB) and patients with suspected glaucoma (MD = -0.30 dB) and early primary open angle glaucoma (POAG) (MD = -2.10 dB). MVD was significantly larger in the healthy subjects than in the patients with suspected glaucoma and POAG patients. Although GCC was significantly different among the three groups, MVD was not different between the patients with suspected glaucoma and those with POAG. These outcomes are partly similar to those obtained in our study. In the current study, we included cases with relatively earlier-stage glaucoma (MD = -3.70 dB), and the narrow range of glaucoma severity may affect the outcome. Two other studies report that mGCC thickness presents a higher AUROC than MVD for differentiating between healthy and moderate glaucomatous eyes (MD = -8.80 dB [24] and - 5.32 dB [25], respectively). Recently, Moghimi S et al. [26] in their cross-sectional study reported the measurement floor and dynamic ranges of OCT and OCT-A in glaucoma with an MD range between 2.8 and -30.1 dB. The estimated floors were 49.5 µm for cpRNFL thickness (measured by Spectralis), 70.7 µm for GCC thickness (measured by Avanti), and 31.2% for circumpapillary VD (measured by AngioVue). MVD reached the estimated floor later in the disease course (VF MD = -25.8 dB) than circumpapillary VD (VF MD = -29.3 dB), cpRNFL thickness (VF MD = -17.5 dB), and GCC thickness (VF MD = -13.9 dB). However, the number of measurement steps from normal values to the estimated floor was greatest for cpRNFL thickness, followed by GCC thickness, circumpapillary VD, and MVD [26]. Although GCC and cpRNFL thickness reached their respective floors earlier along the

glaucoma continuum, thickness parameters to detect glaucomatous changes may be advantageous within their dynamic ranges, especially in early glaucoma. In the current study, multiple regression analysis detected cpRNFL thickness as a significant related factor for MVD in all subjects. However, in glaucomatous eyes, MVD was not statistically different between normal and defective hemifields, despite the difference in IMT, mGCC and cpRNLF thicknesses between the two hemifields. The narrower dynamic range in MVD and the early glaucoma cases included in our study may have affected the outcome.

The present study had several limitations. First, its relatively small sample size might have influenced the results. Second, the regions of interest selected for measurements of MVD, IMT, and GCC thickness were not in direct correspondence because of the limits set by the built-in program provided by each OCT machine manufacturer at the time of data collection.

Furthermore, a potential bias might have been introduced in the anatomy of the measurement area of vessel density. For this study, we measured superficial MVD derived from the superficial capillary plexus, located within the retina between the RNFL and IPL [27, 28]. Although the superficial capillaries mainly nourish the RNFL, RGC layer, and IPL, this superficial plexus has anastomoses with the deep vascular plexus. Thus, a complex network exists for vascular supply to the macula [14, 28]. Third, we did not perform a 10-2 VF test, although both average total TD and average central TD were used in this study. Many studies emphasize the importance of the 10-2 program over the 24-2 or 30-2 programs for improved detection of VF defects at the macula in glaucomatous eyes [11, 29]. Lastly, this was a cross-sectional analysis; thus, we cannot determine whether microvascular change is a primary event or the result of RGC degeneration.

Despite these limitations, this is the first study to use OCT-A to evaluate MVD in NTG eyes with HFD. Another strength of our study is that we only included NTG eyes without systemic diseases or glaucoma medications; this differs from the approaches of other studies [11, 16–18, 21] of glaucoma patients with HFD, which included patients with DM, HT, or a glaucoma medication history. Further, the current study used strict criteria to define a normal VF in healthy subjects and a perimetrically normal hemifield in NTG eyes. Some previous studies defined healthy subjects solely based on optic disc findings.

In conclusion, since reduced thicknesses of the mGCC and cpRNFL as well as changes in MVD, were detected even in the perimetrically normal hemifields of NTG eyes, hemodynamic deficiencies and structural damage might have already begun in these hemifields. Furthermore, in comparison with healthy eyes, MVD was significantly lower in the normal hemifields of NTG eyes, although IMT did not differ between the two groups. Conversely, MVD in NTG eyes was not significantly different between the normal and defective hemifields, despite the difference in IMT between the two hemifields.

Further longitudinal studies including a large numbers of cases with various degrees of disease severity are needed to elucidate whether the reduction in vessel density may precede structural changes early in the disease process, whether the reduction in vessel density is the result of RGC death, whether the reduction in vasculature and structural loss may vary across disease severities or among cases, and whether the differences in the detection powers and dynamic ranges in OCT may affect the outcomes in the macular region.

Acknowledgements Kyoko Ishida reports a grant from JSPS KAKENHI (Grant number JP 26462634).

Conflicts of interest U Nozomu, None; K. Ishida, Grant (JSPS KAKENHI), Lecture fee (Alcon Pharma, Pfizer, Santen, Senju, Otsuka, Kowa, AMO, Sucampo, GlaxoSmithKline, JFC Sales Plan); A. Anraku, Lecture fee (Santen, Alcon Pharma, Kowa, JFC Sales Plan); A. Takeyama, None; G. Tomita, Grant (Alcon Pharma, Pfizer, Santen, Senju, TOPCON CORPORATION, Handaya, Kowa Pharmaceutical, Otsuka, AMO), Lecture fee (Pfizer, Santen, Senju, Otsuka, Japan Focus), Consultant fee (Allergan).

References

1. Weinreb RN, Aung T, Medeiros FA. The pathophysiology and treatment of glaucoma: a review. JAMA. 2014;311:1901–11.
2. Mallick J, Devi L, Malik PK, Mallick J. Update on normal tension glaucoma. J Ophthalmic Vis Res. 2016;11:204–8.
3. Killer HE, Pircher A. Normal tension glaucoma: review of current understanding and mechanisms of the pathogenesis. Eye (Lond). 2018;32:924–30.
4. Razeghinejad MR, Lee D. Managing normal tension glaucoma by lowering the intraocular pressure. Surv Ophthalmol. 2019;64:111–6.
5. Adeghate J, Rahmatnejad K, Waisbourd M, Katz LJ. Intraocular pressure-independent management of normal tension glaucoma. Surv Ophthalmol. 2019;64(1):101–10.
6. Komori S, Ishida K, Yamamoto T. Results of long-term monitoring of normal-tension glaucoma patients receiving medical therapy: results of an 18-year follow-up. Graefes Arch Clin Exp Ophthalmol. 2014;252:1963–70.
7. Van Melkebeke L, Barbosa-Breda J, Huygens M, Stalmans I. Optical coherence tomography angiography in glaucoma: a review. Ophthalmic Res. 2018;60:139–51.
8. Takeyama A, Ishida K, Anraku A, Ishida M, Tomita G. Comparison of optical coherence tomography angiography and laser speckle flowgraphy for the diagnosis of normal-tension glaucoma. J Ophthalmol. 2018;2018:1751857. https://doi.org/10.1155/2018/1751857.eCollection2018.
9. Yarmohammadi A, Zangwill LM, Diniz-Filho A, Suh MH, Yousefi S, Saunders LJ, et al. Relationship between optical coherence tomography angiography vessel density and severity of visual field loss in glaucoma. Ophthalmology. 2016;123:2498–508.
10. Yarmohammadi A, Zangwill LM, Diniz-Filho A, Suh MH, Manalastas PI, Fatehee N, et al. Optical coherence tomography

angiography vessel density in healthy, glaucoma suspect, and glaucoma eyes. Investig Ophthalmol Vis Sci. 2016;57:451–9.
11. Pradhan ZS, Dixit S, Sreenivasaiah S, Rao HL, Venugopal JP, Devi S, et al. A sectoral analysis of vessel density measurements in perimetrically intact regions of glaucomatous eyes: an optical coherence tomography angiography study. J Glaucoma. 2018;27:525–31.
12. Shoji T, Zangwill LM, Akagi T, Saunders LJ, Yarmohammadi A, Manalastas PIC, et al. Progressive macula vessel density loss in primary open-angle glaucoma: a longitudinal study. Am J Ophthalmol. 2017;182:107–17.
13. Moghimi S, Zangwill LM, Penteado RC, Hasenstab K, Ghahari E, Hou H, et al. Macular and optic nerve head vessel density and progressive retinal nerve fiber layer loss in glaucoma. Ophthalmology. 2018;125:1720–8.
14. Penteado RC, Zangwill LM, Daga FB, Saunders LJ, Manalastas PIC, Shoji T, et al. Optical coherence tomography angiography macular vascular density measurements and the central 10-2 visual field in glaucoma. J Glaucoma. 2018;27:481–9.
15. Hou H, Moghimi S, Zangwill LM, Shoji T, Ghahari E, Penteado RC, et al. Macula vessel density and thickness in early primary open angle glaucoma. Am J Ophthalmol. 2019;199:120–32.
16. Chen CL, Bojikian KD, Wen JC, Zhang Q, Xin C, Mudumbai RC, et al. Peripapillary retinal nerve fiber layer vascular microcirculation in eyes with glaucoma and single-hemifield visual field loss. JAMA Ophthalmol. 2017;135:461–8.
17. Akagi T, Iida Y, Nakanishi H, Terada N, Morooka S, Yamada H, et al. Microvascular density in glaucomatous eyes with hemifield visual field defects: an optical coherence tomography angiography study. Am J Ophthalmol. 2016;168:237–49.
18. Yarmohammadi A, Zangwill LM, Diniz-Filho A, Saunders LJ, Suh MH, Wu Z, et al. Peripapillary and macular vessel density in patients with glaucoma and single-hemifield visual field defect. Ophthalmology. 2017;124:709–19.
19. Hou H, Moghimi S, Zangwill LM, Shoji T, Ghahari E, Manalastas PIC, et al. Inter-eye asymmetry of optical coherence tomography angiography vessel density in bilateral glaucoma, glaucoma suspect, and healthy eyes. Am J Ophthalmol. 2018;190:69–77.
20. Anraku A, Ishida K, Enomoto N, Takagi S, Ito H, Takeyama A, et al. Association between optic nerve head microcirculation and macular ganglion cell complex thickness in eyes with untreated normal tension glaucoma and a hemifield defect. J Ophthalmol. 2017;2017:3608396. https://doi.org/10.1155/2017/3608396 Epub 2017 Mar 23.
21. Sehi M, Goharian I, Konduru R, Tan O, Srinivas S, Sadda SR, et al. Retinal blood flow in glaucomatous eyes with single-hemifield damage. Ophthalmology. 2014;12:750–8.
22. Wan KH, Lam AKN, Leung CK. Optical coherence tomography angiography compared with optical coherence tomography macular measurements for detection of glaucoma. JAMA Ophthalmol. 2018;136:866–74.
23. Lommatzsch C, Rothaus K, Koch JM, Heinz C, Grisanti S. OCTA vessel density changes in the macular zone in glaucomatous eyes. Graefes Arch Clin Exp Ophthalmol. 2018;256:1499–508.
24. Chen HS, Liu CH, Wu WC, Tseng HJ, Lee YS. Optical coherence tomography angiography of the superficial microvasculature in the macular and peripapillary areas in glaucomatous and healthy eyes. Investig Ophthalmol Vis Sci. 2017;58:3637–45.
25. Takusagawa HL, Liu L, Ma KN, Jia Y, Gao SS, Zhang M, et al. Projection-resolved optical coherence tomography angiography of macular retinal circulation in glaucoma. Ophthalmology. 2017;124:1589–99.
26. Moghimi S, Bowd C, Zangwill LM, Penteado RC, Hasenstab K, Hou H, et al. Measurement floors and dynamic ranges of OCT and OCT angiography in glaucoma. Ophthalmology. 2019;126:980–8.
27. Iwasaki M, Inomata H. Relation between superficial capillaries and foveal structures in the human retina. Investig Ophthalmol Vis Sci. 1986;27:1698–705.
28. Rutkowski P, May CA. Nutrition and vascular supply of retinal ganglion cells during human development. Front Neurol. 2016;7:49.
29. De Moraes CG, Hood DC, Thenappan A, Girkin CA, Medeiros FA, Weinreb RN, et al. 24-2 visual fields miss central defects shown on 10-2 tests in glaucoma suspects, ocular hypertensives, and early glaucoma. Ophthalmology. 2017;124:1449–56.

Publisher's Note Springer Nature remains neutral with regard to jurisdictional claims in published maps and institutional affiliations.